[gobble]

This manuscript is a non-peer-reviewed preprint submitted to EarthArXiv.

Version 2, 1 September 2026

Changes in Version 2: added an AI-use disclosure statement and data acknowledgements; the scientific content is unchanged from Version 1.

The 26 August 2026 Langtang Lirung ice–rock avalanche and its transboundary cascade: a multi-source observational reconstruction in the Bhote Koshi basin

Donghua Xu (Independent Researcher)

ORCID: https://orcid.org/0009-0003-8256-8416

Corresponding author email: xudonghua.ac@gmail.com

Data cut-off for this version: 31 August 2026, 12:00 UTC.

All data used are openly available; scripts and derived products will be archived at Zenodo (DOI to be assigned).

The 26 August 2026 Langtang Lirung ice–rock avalanche and its transboundary cascade: a multi-source observational reconstruction in the Bhote Koshi basin

Donghua Xu[1*]

[1*]Independent Researcher.

Corresponding author(s). E-mail(s): xudonghua.ac@gmail.com;

Abstract

On 26 August 2026, an ice–rock avalanche detached from the northern flank of Langtang Lirung (7,227 m) at about 5,200 m a.s.l., transformed into a debris flow that travelled roughly 22 km in 6–7 minutes, destroyed the Gyirong border port (China) and dammed the river; a flood then propagated a reported 170 km down the Bhote Koshi–Trishuli–Narayani system into Nepal and India. At least 16 people died in China (546 missing) and 903 bodies were recovered in Nepal (4,247 missing; NDRRMA, 31 August). Using only open data (seismic records, Sentinel-1 SAR backscatter change, emergency mapping, and official reports from both countries), we reconstruct the full cascade and assess the origin of the initial flood wave: it reached the first inhabited stream gauge 12.8 min after the trigger, far too fast to be the overflow of the main barrier lake (began only on 28 August), and was generated by the avalanche-emplaced debris flow and/or a rapid release from the debris dam — indistinguishable with open data. SAR change detection identifies about 7.5 km$^{\mathbf{2}}$ of strongly modified surface in the source sector; assuming 1–5 m affected-layer thickness, this corresponds to a first-order volume-equivalent scale of $\sim 10^{\mathbf{7}}$ m$^{\mathbf{3}}$, not a direct estimate of the detached source volume. ERA5-Land shows a modest warm anomaly (+0.59 K, July–August 2026 vs. 1991–2020). The event recurred at the same transboundary site 14 months after the July 2025 Gyirong glacial lake outburst flood, highlighting slope-scale monitoring and cross-border data sharing as priorities.

Keywords: ice–rock avalanche, debris flow, barrier lake, river damming, flood cascade, transboundary hazard, High Mountain Asia, Langtang Lirung, Bhote Koshi

1 Introduction

Cryospheric hazards in High Mountain Asia (HMA) have intensified over the past two decades, driven by rapid warming, glacier recession and permafrost degradation [1, 2]. Beyond the widely studied glacial lake outburst floods (GLOFs) [3–5], a growing class of events originates from the detachment of ice and ice–rock masses from steep glacierised slopes, producing ice–rock avalanches that can transform into long-runout debris flows and, in some cases, flood cascades [6–8]. The 7 February 2021 Chamoli event (India), in which a $\sim 27 \times 10^6$ m^3 rock–ice avalanche generated a debris flow that destroyed two hydropower plants and killed more than 200 people [6], exemplifies this hazard class; the October 2023 Sikkim flood cascade [9, 10], the 2021 Melamchi erosional cascade [11], the 2024 Thame GLOF [12, 13] and the 2000 Yigong rockslide-dam outburst [14, 15] illustrate how small trigger volumes can amplify into transboundary disasters through erosion and damming processes [16–18].

On 26 August 2026, a new and larger-scale example of such a cascade struck the China–Nepal border region. An ice–rock avalanche from the northern flank of Langtang Lirung (7,227 m) at ∼5,200 m a.s.l. transformed into a high-speed debris flow that reached the Gyirong (Jilong) border port, Xizang (Tibet), China, within 6–7 minutes, destroyed about 0.7 km^2 of the port area, and dammed the river; a flood then propagated a reported 170 km downstream along the Bhote Koshi (Rasuwa)–Trishuli–Narayani corridor into Nepal and India. As of 29 August 2026, Chinese authorities reported 16 dead and 546 missing (including 261 foreign nationals from 23 countries); Nepal's National Disaster Risk Reduction and Management Authority (NDRRMA) reported 903 bodies recovered and 4,247 missing on 31 August. The event has been variously described in the literature and media as the "Bhotekoshi flash flood" [19], the "Gyirong mudslide" (Chinese official statements) and the "2026 Nuwakot Flood"; here we adopt the term *the 26 August 2026 Gyirong–Bhote Koshi ice–rock avalanche cascade*.

The disaster occurred only 14 months after the 8 July 2025 Gyirong GLOF at the same border location [20, 21], which was attributed to a supraglacial lake outburst on the upper Purepu Tsangpo and caused at least nine fatalities and the temporary closure of the port. The repeated, mechanism-distinct cryospheric failure at one transboundary site raises urgent questions about monitoring, warning and data-sharing between the two countries [22, 23].

Early scientific responses to the 2026 event include a rapid analysis report by the International Research on Disaster Risk (IRDR) [24], a preliminary investigation by the Chinese national key laboratory [25], and a preprint (not peer reviewed) that quantified the warning chain, showing that the public alert followed the trigger by 38.8 min while the flood wave reached the first inhabited gauge in 12.8 min, implying a negative lead time of 26 min [19]. To date, no peer-reviewed study has provided a full multi-source reconstruction of the cascade from the source area to the downstream flood, nor assessed the origin of the initial flood wave or the relationship between the 2025 and 2026 events at the same site.

This study addresses three research questions: **RQ1** how can the cascade chain (source area, flow path, damming, breach, flood propagation) be reconstructed from open multi-source observations? **RQ2** what were the trigger and environmental conditions (meteorological anomalies, absence of tectonic triggering)? **RQ3** what generated the initial flood wave on 26 August — the avalanche-emplaced flow itself (H1), a rapid partial breach of the debris dam (H2), or the later overflow of the main barrier lake (H3)?

2 Study area and event setting

2.1 Geographic setting

Langtang Lirung (7,227 m) is the highest peak of the Langtang Himal, Nepal, about 30 km north of Kathmandu and immediately south of the China–Nepal border. Its northern flank drains via the Chhochen Khola (also reported as Lhende Khola [19]) into the Purepu Tsangpo (also reported as Donglin Zangbo in Chinese official accounts; Zhang et al. [20] describe the upper Purepu Tsangpo as a tributary of the Donglin Tsangpo), which crosses the border at the Gyirong port and becomes the Bhote Koshi in Rasuwa District, Nepal. The Bhote Koshi joins the Trishuli at Nuwakot; the Trishuli–Narayani (Gandaki) system continues to the Ganges lowlands of India, a reported 170 km downstream of the source area. We use the nomenclature of the official Xizang press conference for Chinese-side streams and note the alternative names where they occur in the literature. The Bhote Koshi (Rasuwa) studied here is distinct from the Bhotekoshi river of the Sun Koshi system (Kodari), which was the site of the July 2016 flood [26].

2.2 Precursor event: the 8 July 2025 Gyirong GLOF

On 8 July 2025, a GLOF originating from a supraglacial lake on the upper Purepu Tsangpo inundated the same border corridor. Remote-sensing analysis [20] documented a $\sim$45% (0.31 km^2) decrease of the lake area, a $\sim$7.65-fold expansion between 9 May and 6 July 2025 (from $\sim$0.08 to $\sim$0.69 km^2; the ratio implied by the reported values is $\sim$8.6, indicating rounding in the source), and downstream peak discharge amplification to about 8,400 m^3 s^{-1} ($\approx$6-fold) in narrow, V-shaped downstream reaches. The flood caused at least nine deaths and left 19 people missing (peer-reviewed estimate [20]; early media reports gave lower rolling counts), damaged the port and led to its temporary closure. A companion study [21] highlighted precursor signals and monitoring gaps.

2.3 Data cut-off

The data cut-off for this version is **31 August 2026, 12:00 UTC**. Facts and figures in this paper reflect information available up to that time; later developments are treated in Section 4.5 as post-event evolution and will be incorporated in subsequent versions of this preprint.

3 Data and methods

3.1 Seismic records

We queried the USGS ComCat FDSN event service for the region 27.5–29.5°N, 84.5–86.5°E for 2026 and verified that no M≥4 tectonic earthquake occurred prior to the event. Two events were recorded on 26 August: M5.2 at 02:52:10 UTC (10:52:10 Beijing time) and M4.2 at 06:00:35 UTC, both classified as landslide-type with 0 km depth. The Italian National Institute of Geophysics and Volcanology (INGV) explicitly clarified that the signal was generated by the avalanche and dam-breach processes, not by an earthquake. We therefore treat the M5.2 signal as the avalanche origin time.

3.2 Sentinel-1 SAR backscatter change detection

We used Sentinel-1 IW GRD images (dual-polarisation VV/VH, descending orbit) from Google Earth Engine. The VV backscatter values in the COPERNICUS/S1_GRD collection are in decibels (log scaling); we therefore quantify change as the difference ΔdB = post − pre. The pre-event state is the median of six scenes acquired 26 July–24 August 2026; the post-event state is the single available descending scene of 31 August 2026 (the 12-day revisit cycle and monsoon conditions limited post-event coverage; scene counts were verified against the collection). Areas with $\Delta\text{dB} < -3$ dB (backscatter decrease, consistent with erosion or removal of surface material) and $> +3$ dB (increase, consistent with deposition or standing water) were mapped at 10-m pixel spacing; the analysis region is limited to the source sector east of ∼85.4°E where post-event coverage is valid. Statistics were computed with a documented script (pixel-to-area conversion at the AOI latitude); we note that seasonal surface change (early-season snow) cannot be fully excluded [27].

3.3 Optical baseline

The lowest-cloud pre-event Sentinel-2 L2A scene of 24 August 2026 (tile 45RUM, 38.6% cloud cover; 29.1% for the L1C product) provides the pre-event surface context. Post-event cloud-free optical coverage was unavailable (monsoon conditions), so post-event mapping relies on SAR and emergency mapping products.

3.4 Emergency mapping and flood extent

We used the Copernicus Emergency Management Service (EMS) activation EMSR927 grading products for three areas of interest (AOI01–03) [28], the HOT/OSM flood extent observed on 27 August 2026 (31.7 km^2), and OSM waterways for cartography. EMSR927 grading includes damaged infrastructure (e.g., Trishuli Power House, Rasuwagadhi hydropower dam, Langtang Khola hydroelectric plant; road damage in AOI03 including 613 segments of the Pasang Lhamu Highway); building counts (433/431/2,343 in AOI01/02/03) and road-segment counts were verified by direct count from the delivered shapefiles.

3.5 Meteorological reanalysis

We use ERA5-Land [29] daily 2-m temperature for July and August 2026 against the 1991–2020 climatology to test the reported "warmest surface temperatures in two years" prior to the collapse; the anomaly results are presented in Section 4.4.

3.6 Official data and ethics

We rely on official statements of the Xizang Autonomous Region press conference (30 August 2026), the Ministry of Water Resources radar survey of the barrier lake, NDRRMA situation reports, and the USGS/INGV statements. Casualty figures are quoted with their reporting date. This study uses only openly available data; no individuals are identified; no funding was received.

4 Results

4.1 Source area and flow path

The seismic record places the avalanche origin at 02:52:10 UTC on 26 August 2026 (10:52:10 Beijing time), consistent with the official timeline. The preliminary investigation [25] reports an ice–rock avalanche of about 88 s duration from the northern flank of Langtang Lirung at ∼5,200 m a.s.l., followed by a debris flow that travelled ∼22 km over a vertical drop of ∼3,300 m and impacted the Gyirong port (∼1,800 m) at 10:59 Beijing time, i.e., within 6–7 minutes (mean speed of order 50 m s^{-1}; the China Geological Survey reports "7 minutes, 20 km").

Sentinel-1 backscatter change (VV, ΔdB = post minus pre; six pre-event scenes, 26 July–24 August, versus the single post-event scene of 31 August; descending orbit) reveals a strongly modified surface zone ($\Delta dB < -3$ dB) of about 7.5 km^2 within the source window (85.44–85.50°E, 28.28–28.34°N) (Fig. 3); across the full valid analysis sector, 53 km^2 show a decrease and 27 km^2 an increase. The mapped change area may include, in addition to source detachment, erosion along the flow path, debris deposition, wet-snow/seasonal surface change and SAR geometry and soil-moisture effects; it should not be interpreted as a direct measure of the detached source area. Under an assumed equivalent affected-layer thickness of 1–5 m, the mapped change corresponds to a first-order volume-equivalent scale of $\sim 10^7$ m^3 ($1–4\times10^7$ m^3), not a direct estimate of the detached source volume. No post-event cloud-free optical imagery was available (monsoon); the pre-event Sentinel-2 scene of 24 August 2026 serves as baseline context (Fig. 3).

4.2 River damming and barrier lakes

The debris flow dammed the river at the confluence of the Chhochen Khola with the Purepu Tsangpo, upstream of the port. The Ministry of Water Resources radar survey characterised the main barrier dam as ∼60 m high, ∼1,100 m long and ∼300 m wide, impounding a lake of ∼0.1 km^2 with a volume of $\sim 2.2\times10^6$ m^3. A second, smaller suspected barrier lake was identified about 5 km upstream, near the source area, by the PowerChina-1 X-band SAR satellite on 28 August. The main lake began to overflow on 28 August at 17:50 Beijing time (outflow $\sim$50 m^3 s^{-1} vs. inflow $\sim$23 m^3 s^{-1}) and was largely drained naturally by 29–30 August. At the reported inflow, the reported volume would accumulate in about 27 h — of the same order as the $\sim$63 h observed between damming and the reported overflow onset — suggesting seepage, lower initial inflow, or uncertainty in the reported parameters.

4.3 Flood propagation

The initial flood wave reached the first inhabited stream gauge of Nepal's Flood Forecasting Division in 12.8 min after the trigger [19], i.e., before any significant barrier-lake storage could have accumulated. Satellite-based flood mapping (HOT, observed 27 August) delineated 31.7 km^2 of inundated area along the Bhote Koshi–Trishuli corridor. Copernicus EMSR927 grading documents damage along the corridor: 433 buildings assessed in the upper Bhote Koshi valley (AOI01), 431 near Rasuwagadhi (AOI02) and 2,343 around Bidur on the Trishuli (AOI03), plus hydropower infrastructure (Trishuli Power House, Rasuwagadhi hydropower dam, Langtang Khola plant; $\sim$748 MW of capacity affected, 354 MW operational and 394 MW under construction, per the IRDR rapid assessment [24]), bridges and the Pasang Lhamu Highway (613 damaged segments in AOI03; counts verified by direct count from the delivered shapefiles). Reported flood impacts extend about 170 km downstream to the Narayani/Gandak system at the India border [22]. Official casualty figures as of the data cut-off are 16 dead and 546 missing on the Chinese side (29 August, including 261 foreign nationals from 23 countries) and 903 bodies recovered with 4,247 missing in Nepal (NDRRMA, 31 August).

4.4 Trigger and environmental conditions

No $M \geq 4$ tectonic earthquake occurred in the region during 2026 before the event (USGS catalog; verified 31 August 2026), and INGV confirmed the recorded signals were generated by the mass movement itself. The event therefore was not seismically triggered. ERA5-Land shows a modest positive anomaly of +0.59 K in mean 2-m temperature for July–August 2026 relative to the 1991–2020 climatology over the study region, with daily values of 9.3–11.3 °C in the valley; the media-reported "warmest surface temperatures in two years" claim is not strongly supported at this spatial scale, although reanalysis uncertainty in steep terrain is large (Fig. 5). Rainfall preceding the event has been reported but its quantitative contribution remains to be assessed.

4.5 Post-event evolution

After this data cut-off (31 August 2026, 12:00 UTC), the barrier lake remained drained and rescue operations continued on both sides of the border; the official figures quoted above may be updated in subsequent versions of this preprint if authorities release definitive numbers.

5 Discussion

5.1 A cascade chain consistent across independent observations

The multi-source observations are mutually consistent: the seismic origin time (02:52:10 UTC), the official impact time at the port (02:59 UTC), the 12.8-min arrival at the first gauge [19], the 88-s avalanche duration [25], the barrier-lake parameters and overflow timing (28 August), and the flood extent mapped on 27 August jointly constrain a single cascade: ice–rock avalanche → debris flow → river damming → breach/overflow flood → 170-km downstream propagation. The event shares the generic structure of the Chamoli cascade [6] and of rockslide-dam outburst floods [14, 16], but differs in its transboundary impact and in the short warning time available [19]. The first-order volume-equivalent scale ($\sim 10^7$ m^3; see Section 4.1 for the associated caveats) is comparable to the 27×10^6 m^3 Chamoli detachment [6]; the downstream impact was modulated here by the damming–breach sequence and by the steep, constricted valley that funnelled the flow into the border port.

5.2 RQ3: origin of the initial flood wave

Three scenarios for the initial flood wave (26 August) were evaluated: (H1) the avalanche-emplaced debris flow itself generated the wave; (H2) a rapid partial breach of the debris dam released stored water within minutes to hours; (H3) the main barrier lake overflow (28 August 17:50) generated the wave. The evidence excludes H3 as the source of the initial wave: the wave reached the first inhabited gauge 12.8 min after the trigger [19], far too fast for a lake-fill-and-overflow process; the flood extent was already observable on 27 August; and overflow began only on 28 August. The timing alone, however, cannot separate H1 from H2: a rapid partial release of impounded water within minutes of damming would arrive at the gauges on the same timescale as the emplaced flow. Moreover, the official INGV clarification describes exactly such a mechanism — temporary blockage of the river by debris followed by breaching of the natural dam and release of water, mud and debris [30]. The energy budget of the preprint [19] ($\sim$19.96 $\times 10^6$ m^3 excess volume, with frictional meltwater excluded as the sole source) is likewise consistent with a substantial water-release component. We therefore conclude that the initial wave was generated within minutes of avalanche emplacement by the emplaced debris flow and/or a rapid release from the debris dam (H1/H2), that H3 is excluded, and that the relative contributions of H1 and H2 cannot be separated with openly available data; gauge-level records from both countries would be required. The 28 August overflow of the main barrier lake constituted a later, secondary flood wave.

5.3 Two cryospheric disasters at one transboundary site

The 2025 GLOF [20, 21] and the 2026 ice–rock avalanche cascade (Table 2) originated from different mechanisms (lake outburst vs. glacier detachment), yet both produced catastrophic downstream impacts at the same port and valley, 14 months apart. This recurrence demonstrates that monitoring strategies focused only on glacial lakes [3, 4, 31] are insufficient: glacierised slopes above the valleys must also be monitored

[7, 8, 32]. It also underscores the value of multi-hazard transboundary risk assessment [23, 33, 34].

5.4 Early warning and governance gaps

The quantified warning latency of the 2026 event — mass alert 38.8 min after the trigger vs. 12.8 min flood travel time to the first inhabited gauge (timing figures from the preprint [19], not peer reviewed, based on the seismic origin time and the gauge chronology of Nepal's Flood Forecasting Division) — implies that even a well-functioning national warning chain could not have provided lead time at the uppermost gauges [19, 22]. Our reconstruction adds that the destruction of the two uppermost gauges at 27% and 87% of their warning stages (reported in the same preprint) left threshold-based systems blind. Cross-border data sharing (seismic, gauge, satellite) and slope-scale monitoring are the actionable gaps identified by this event and its 2025 precursor.

5.5 Discrepancy with the IRDR rapid assessment

The IRDR rapid analysis report [24], prepared within days of the event from early secondary data, proposed a different chronology: an ice–rock–soil mass failure on 25 August 2026 (13:00–14:00 Nepal time), formation of a temporary natural dam lasting approximately 18–19 h, and a dam breach at 08:30–08:37 Nepal time on 26 August, which it associated with the recorded seismic signal. This chronology cannot be reconciled with the one adopted here. First, the official Xizang press conference and the China Geological Survey place the avalanche initiation at 10:52 Beijing time (08:37 Nepal time) on 26 August and the impact at the Gyirong port 6–7 min later; had the mass failure occurred on 25 August, the port would have been affected a day earlier, contradicting all contemporaneous reports. Second, the seismic signal (M5.2, landslide type, 0 km depth) coincides with the 08:37 Nepal time initiation and with ground reports of a loud roar at the same minute [30]; the INGV clarification describes blockage followed by a rapid release — i.e., the signal brackets a single event on the morning of 26 August, not a breach after an 18–19 h impoundment. Third, the initial flood wave reached the first inhabited gauge within 12.8 min of 08:37 Nepal time [19] and devastated Timure during the day on 26 August; a breach 18–19 h after a 25 August failure would have produced the flood during the night of 25–26 August, inconsistent with the observed timing. The IRDR report itself notes that its reconstruction relied on preliminary secondary data and that tributary inflow may have masked the upstream blockage, which may explain the earlier dating. We therefore retain the official/INGV chronology (initiation at 08:37 Nepal time on 26 August) while acknowledging that both assessments share the same core mechanism (blockage followed by rapid release) and that resolving the residual timing uncertainty requires gauge and seismic waveform records from both countries. Note that the IRDR interpretation of the 08:37 signal as a breach rather than an initiation does not affect our RQ3 conclusion: under either reading, the initial flood wave was released abruptly within minutes to hours of damming — not by the slow overflow of the main barrier lake on 28 August.

5.6 Limitations

(1) No public post-event high-resolution DEM was available at the time of analysis; the SAR change area cannot be converted into a direct volume estimate, and only a first-order volume-equivalent scale ($\sim 10^7$ m^3, source sector, under an assumed affected-layer thickness of 1–5 m) is reported; seasonal surface change cannot be fully excluded. (2) Post-event optical imagery was unavailable because of monsoon cloud cover; SAR backscatter analysis partially compensates, but the post-event SAR coverage is a single scene (31 August) restricted to the source sector, leaving the port area without SAR change detection (the port is covered instead by EMSR927 grading and official reports). (3) Gauge records from Nepal's Flood Forecasting Division were not directly accessible to us; timing figures rely on the preprint [19]. (4) Casualty figures are evolving and are quoted with dates. (5) ERA5 anomaly values carry substantial uncertainty in steep terrain and should be treated as indicative.

6 Conclusion

We reconstructed the 26 August 2026 Gyirong–Bhote Koshi ice–rock avalanche cascade from open multi-source observations. The cascade chain is consistent across seismic, SAR, emergency-mapping and official data: an ice–rock avalanche of about 88 s from the northern flank of Langtang Lirung at $\sim$5,200 m a.s.l., a debris flow covering $\sim$22 km in 6–7 min that destroyed the Gyirong port and dammed the river, and a flood that propagated a reported 170 km into Nepal and India. The initial flood wave arrived within $\sim$13 min of the avalanche — far before the main barrier lake began to overflow on 28 August — and was generated by the avalanche-emplaced debris flow and/or a rapid release from the debris dam, which cannot be separated with open data. SAR change detection constrains the strongly modified surface area in the source sector to $\sim$7.5 km^2, corresponding under an assumed affected-layer thickness of 1–5 m to a first-order volume-equivalent scale of $\sim 10^7$ m^3 (not a direct estimate of the detached source volume). The recurrence of two mechanistically distinct cryospheric disasters at the same transboundary site within 14 months — a GLOF in July 2025 and an ice–rock avalanche cascade in August 2026 — highlights slope-scale monitoring and cross-border data sharing as the priorities for reducing future risk in this corridor.

Declarations

- **Use of AI tools**: During the preparation of this work the author used artificial-intelligence tools (large language models and automated code assistants) for literature search and synthesis, data processing and figure generation, and for drafting and editing assistance. After using these tools, the author reviewed and verified the content, data and code, and takes full responsibility for the content of the publication. No AI tool was used to generate or alter research data.
- **Preprint**: An earlier version of this manuscript is available as a non-peer-reviewed preprint on EarthArXiv: https://doi.org/10.31223/X56793.
- **Funding**: No funding was received for this study.
- **Conflict of interest**: The author declares no conflict of interest.

- **Data availability**: All data used are openly available: USGS ComCat, Copernicus Data Space (Sentinel-1/2), Copernicus EMS EMSR927 (HDX), HOT/OSM (HDX), ERA5-Land (Copernicus CDS); official statements as cited. Processing scripts and derived products are archived at Zenodo: https://doi.org/10.5281/zenodo.22217602. Additional links are provided in this article's supplementary information.

Acknowledgements

The author gratefully acknowledges the open data and public statements used in this work: the Copernicus Emergency Management Service (activation EMSR927) and Copernicus Sentinel data (2026), the Humanitarian OpenStreetMap Team and OpenStreetMap contributors (ODbL), the European Centre for Medium-Range Weather Forecasts (ERA5-Land), the US Geological Survey (ComCat) and the Istituto Nazionale di Geofisica e Vulcanologia (INGV), the National Disaster Risk Reduction and Management Authority of Nepal (NDRRMA), and the authorities of Xizang Autonomous Region, China, for their press conferences and official statements. Processing was carried out with Google Earth Engine and free software.

7 Tables and figures

Table 1 Key parameters of the 26 August 2026 Gyirong–Bhote Koshi ice–rock avalanche cascade. Casualty figures are quoted with their reporting date.

Parameter	Value	As of
Avalanche initiation	26 Aug 2026, 10:52:10 Beijing time (02:52:10 UTC); M5.2 seismic signal, landslide type, 0 km depth (USGS; initially reported as M4.4, revised)	26 Aug
Source	Langtang Lirung (7,227 m) northern flank, ∼5,200 m a.s.l.	30 Aug
Avalanche duration	∼88 s	29 Aug
Debris-flow runout	∼22 km in 6–7 min; drop ∼3,300 m	29–30 Aug
Impact at Gyirong port	∼0.7 km^2, 27 structures; G216, power, telecom	26 Aug
Main barrier lake	Dam 60 m × 1,100 m × 300 m; lake 0.1 km^2; ∼2.2×10^6 m^3	28–30 Aug
Overflow onset	28 Aug 17:50 (outflow 50 vs inflow 23 m^3 s^{-1})	30 Aug
Lake drainage	Largely drained by 29–30 Aug	30 Aug
Flood propagation	Bhote Koshi–Trishuli–Narayani, reported ∼170 km to India	26–31 Aug
Casualties, China	16 dead, 546 missing (261 foreign, 23 countries)	29 Aug 18:00
Casualties, Nepal	903 bodies, 4,247 missing (NDRRMA)	31 Aug 09:00
Tectonic trigger	None (no M≥4 tectonic event in 2026 before the event; INGV clarification)	31 Aug

Table 2 Comparison of the two cryospheric disasters at the same transboundary site.

Aspect	8 Jul 2025 Gyirong GLOF	26 Aug 2026 Gyirong–Bhote Koshi cascade
Mechanism	Supraglacial lake outburst (GLOF)	Ice–rock avalanche, debris flow, damming, breach flood (non-GLOF)
Source	Supraglacial lake, upper Purepu Tsangpo	Langtang Lirung northern flank, ∼5,200 m
Source-scale signal	Lake area -0.31 km^2 (-45%); 7.65× expansion 9 May–6 Jul 2025	∼88 s avalanche; debris flow ∼22 km in 6–7 min
Peak discharge	∼8,400 m^3 s^{-1} (downstream, ≈6× amplification)	Not gauged; first gauge hit in ∼12.8 min
Impact	≥9 dead, 19 missing; port closed	China: 16 dead, 546 missing; Nepal: 903 bodies, 4,247 missing (NDRRMA)
Warning	—	No alert before arrival; mass alert 38.8 min after trigger
Interval	—	14 months

References

[1] Khadka, N., Chen, X., Sharma, S., Shrestha, B.: Climate change and its impacts on glaciers and glacial lakes in nepal himalaya. Regional Environmental Change **23**, 143 (2023) https://doi.org/10.1007/s10113-023-02142-y

[2] Shrestha, F., *et al.*: Enhanced glacial lake activity threatens numerous communities and infrastructure in the third pole. Nature Communications **14**, 8250 (2023) https://doi.org/10.1038/s41467-023-44123-z

[3] Cook, K.L., Andermann, C., Gimbert, F., Adhikari, B.R., Hovius, N.: Glacial lake outburst floods as drivers of fluvial erosion in the himalaya. Science **362**(6410), 53–57 (2018) https://doi.org/10.1126/science.aat4981

[4] Zhang, T., *et al.*: An integrative method for identifying potentially dangerous glacial lakes in the himalayas. Science of the Total Environment **806**, 150442 (2022) https://doi.org/10.1016/j.scitotenv.2021.150442

[5] Adhikary, S., Pradhananga, D., Marahatta, S.: Glacial lake outburst floods (glofs) in the nepal himalayas: Recent events, urgent response, and global actions for cryospheric science. Journal of Tourism and Himalayan Adventures **7**(1), 88–92 (2025) https://doi.org/10.3126/jtha.v7i1.80915

[6] Shugar, D.H., Jacquemart, M., Shean, D., *et al.*: A massive rock and ice avalanche caused the 2021 disaster at chamoli, indian himalaya. Science **373**(6552), 300–306 (2021) https://doi.org/10.1126/science.abh4455

[7] Kääb, A., Jacquemart, M., Gilbert, A., Leinss, S., Girod, L., Huggel, C., Falaschi, D., Ugalde, F., Petrakov, D., Chernomorets, S., Dokukin, M., Paul, F., Gascoin, S., Berthier, E., Kargel, J.S.: Sudden large-volume detachments of low-angle mountain glaciers – more frequent than thought? The Cryosphere **15**(4), 1751–1785 (2021) https://doi.org/10.5194/tc-15-1751-2021

Fig. 1 Study area and event chain. Flood extent observed 27 August 2026 (HOT/OSM); Copernicus EMSR927 areas of interest; OSM waterways; DEM: Copernicus DEM 30 m. Placemarks of source area and barrier lake are approximate.

[8] Vries, M., Bhushan, S., Jacquemart, M., Deschamps-Berger, C., Berthier, E., Gascoin, S., Shean, D.E., Shugar, D.H., Kääb, A.: Pre-collapse motion of the february 2021 chamoli rock–ice avalanche, indian himalaya. Natural Hazards and Earth System Sciences **22**(10), 3309–3327 (2022) https://doi.org/10.5194/nhess-22-3309-2022

[9] Sattar, A., Cook, K.L., Rai, S.K., Berthier, E., Allen, S., Rinzin, S., Vries, M., Haeberli, W., Kushwaha, P., Shugar, D.H., *et al.*: The sikkim flood of october 2023: Drivers, causes, and impacts of a multihazard cascade. Science **387**(6740), 2659 (2025) https://doi.org/10.1126/science.ads2659

[10] Mohanty, L.K., Gantayat, P., Dixit, A., Das Adhikari, M., Biswas, R., Singh, V.K.: Sequence of events that led to the south lhonak lake outburst flood in sikkim, india. Scientific Reports **16**, 9741 (2026) https://doi.org/10.1038/

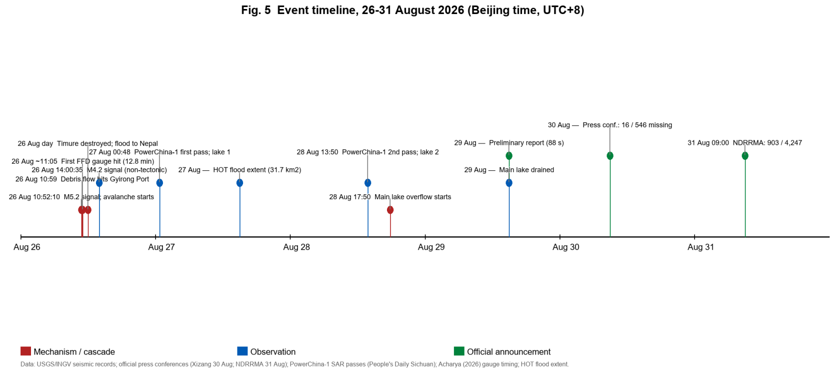

Fig. 2 Event timeline, 26–31 August 2026 (Beijing time), with mechanism, observation and official-announcement events.

s41598-026-35895-7

[11] Chen, C.-M., Hollingsworth, J., Clark, M.K., Chamlagain, D., Bista, S., Zekkos, D., Siwakoti, A., West, A.J.: Erosional cascade during the 2021 melamchi flood. Nature Geoscience **17**, 32–36 (2024) https://doi.org/10.1038/s41561-024-01596-x

[12] Maharjan, S.B., Sherpa, T.C., Shrestha, A.B.: Thame valley glacial lake outburst flood – causes, impacts, and future risks. Technical report, International Centre for Integrated Mountain Development (ICIMOD) (October 2025). https://radionepalonline.com/en/2025/10/26/418818.html

[13] Sharma, K., Strouth, A., Mark, E., Hille, M.: The himalayan hazard: Post-event assessment of thame glacial lake outburst flood in everest region, nepal. Asian Journal of Engineering Geology **2**(Special Issue (ARC-15 of IAEG)), 405–406 (2025)

[14] Delaney, K.B., Evans, S.G.: The 2000 yigong landslide (tibetan plateau), rockslide-dammed lake and outburst flood: Review, remote sensing analysis, and process modelling. Geomorphology **246**, 377–393 (2015) https://doi.org/10.1016/j.geomorph.2015.06.020

[15] Hu, K., Wu, C., Wei, L., Zhang, X., Zhang, Q., Liu, W., Yanites, B.J.: Geomorphic effects of recurrent outburst superfloods in the yigong river on the southeastern margin of tibet. Scientific Reports **11** (2021) https://doi.org/10.1038/s41598-021-95194-1

[16] Costa, J.E., Schuster, R.L.: The formation and failure of natural dams. Geological Society of America Bulletin **100**(7), 1054–1076 (1988) https://doi.org/10.1130/0016-7606(1988)100⟨1054:TFAFON⟩2.3.CO;2

[17] Carrivick, J.L., Tweed, F.S.: A global assessment of the societal impacts of glacier

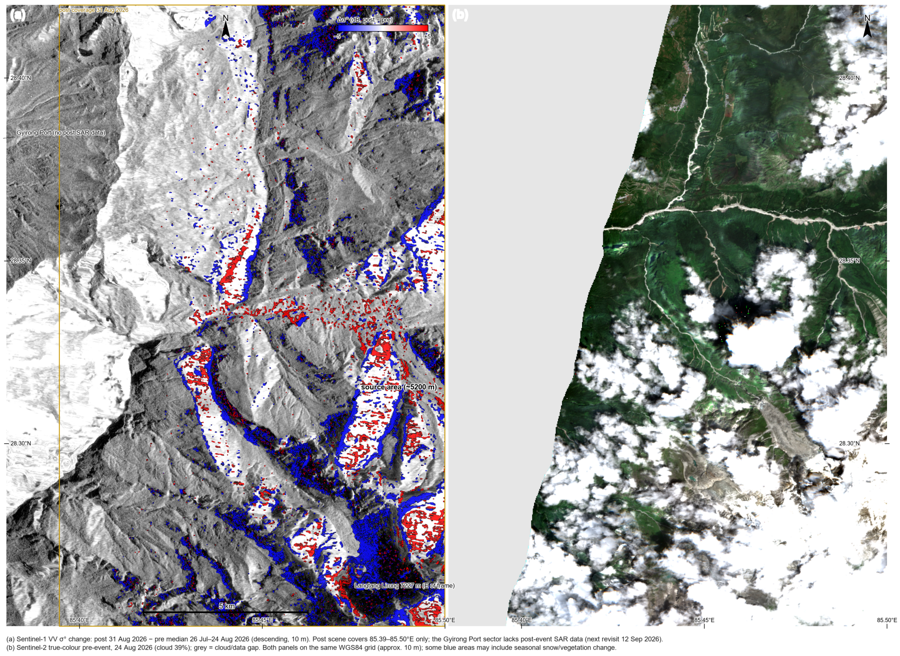

Fig. 3 Sentinel-1 backscatter change (ΔdB, VV) in the source sector (left; blue-white-red) and pre-event Sentinel-2 baseline of 24 August 2026 (right). Post-event SAR coverage is a single descending scene of 31 August; the change analysis is limited to the source sector east of ∼85.4°E.

outburst floods. Global and Planetary Change **144**, 1–16 (2016) https://doi.org/10.1016/j.gloplacha.2016.07.001

[18] Iverson, R.M., Reid, M.E., Logan, M., LaHusen, R.G., Godt, J.W., Griswold, J.P.: Positive feedback and momentum growth during debris-flow entrainment of wet bed sediment. Nature Geoscience **4**, 116–121 (2011) https://doi.org/10.1038/ngeo1040

[19] Acharya, S.: The Bhote Koshi–Trishuli flash flood of 26 August 2026, Rasuwa, Nepal: warning latency exceeded flood travel time. EarthArXiv preprint (version 3) (2026). https://doi.org/10.31223/X5HN5H . https://eartharxiv.org/repository/view/14687/

[20] Zhang, Q., Hu, K., Liu, S., Wei, L., Zhang, X.: Remote sensing interpretation of causes and dynamics of the gyirong outburst flood disaster, tibet, on july 8, 2025. Natural Hazards **122**(7) (2026) https://doi.org/10.1007/s11069-026-08081-1

[21] Peng, D., et al.: Small lakes, catastrophic impacts: Precursor signals and monitoring gaps revealed by the 2025 gyirong glof. Geomorphology (2026)

[22] Thakuri, S.: Early warning could have saved hundreds of lives in nepal floods.

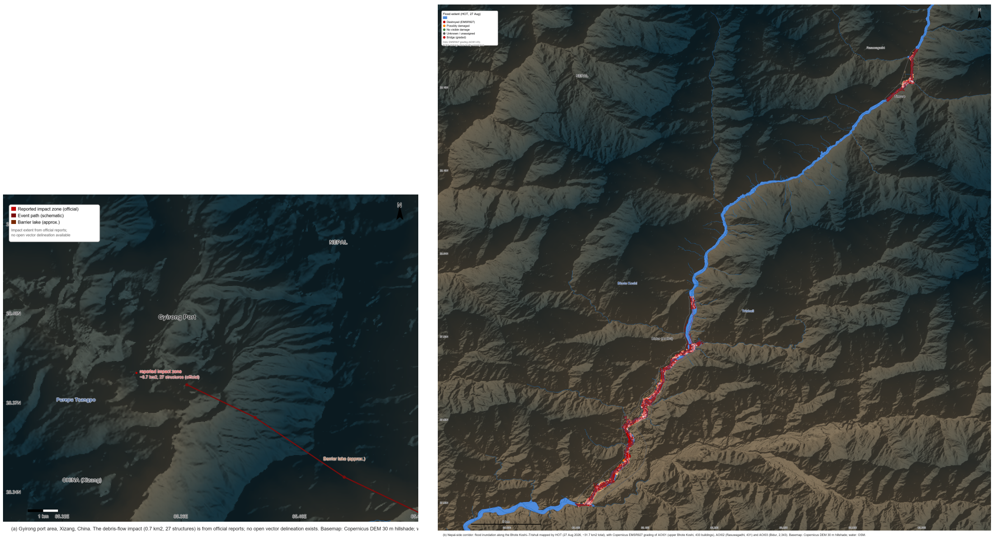

Fig. 4 Flood impacts: (a) Gyirong port area, Xizang — the debris-flow impact (~0.7 km^2, 27 structures) is from official reports; no open vector delineation exists (event path schematic). (b) Nepal-side corridor — flood inundation along the Bhote Koshi–Trishuli mapped by HOT (27 August 2026, 31.7 km^2 total), with Copernicus EMSR927 grading of AOI01 (upper Bhote Koshi, 433 buildings), AOI02 (Rasuwagadhi, 431) and AOI03 (Bidur, 2,343; AOI01 damage class mostly unassigned). Basemap: Copernicus DEM 30 m hillshade; water: OSM.

Nature India (2026) https://doi.org/10.1038/d44151-026-00167-w

[23] Lamichhane, S., Aryal, K.R., Talchabhadel, R., Thapa, B.R., Adhikari, R., Khanal, A., Pandey, V.P., Gautam, D.: Assessing the prospects of transboundary multihazard dynamics: The case of bhotekoshi–sunkoshi watershed in sino–nepal border region. Sustainability **13**(7), 3670 (2021) https://doi.org/10.3390/su13073670

[24] Integrated Research on Disaster Risk (IRDR): IRDR Rapid Analysis Report – Scientific Anatomy of the 26 August 2026 Bhotekoshi Flash Flood – Nepal. ReliefWeb (UNDRR) (2026). https://reliefweb.int/report/nepal/irdr-rapid-analysis-report-scientific-anatomy-26-august-2026-bhotekoshi-flash-flood

[25] National Key Laboratory of Geological Hazard Prevention and Geological Environment Protection: Preliminary investigation report on the Jilong (Gyirong) debris-flow disaster. Released 29 August 2026; republished by Tencent News and Phoenix News (2026). https://news.qq.com/rain/a/20260829A0AD3O00

[26] Sattar, A., Haritashya, U.K., Kargel, J.S., Karki, A.: Transition of a small himalayan glacier lake outburst flood to a giant transborder flood and debris flow. Scientific Reports **12**, 12421 (2022) https://doi.org/10.1038/s41598-022-16337-6

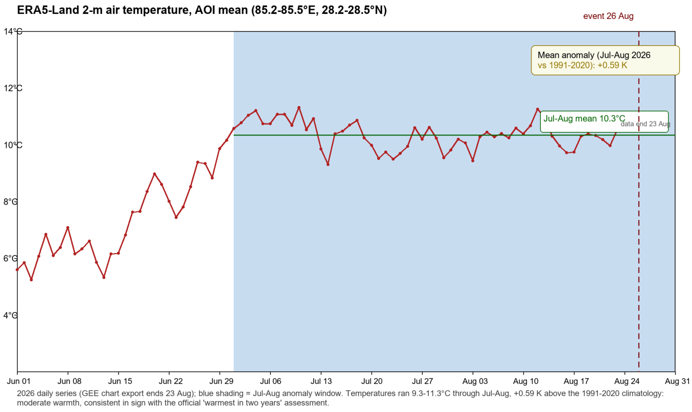

Fig. 5 ERA5-Land 2-m temperature for June–August 2026 over the study area (upper panel: daily series; lower panel: anomaly map July–August 2026 vs. 1991–2020 climatology). Mean anomaly +0.59 K.

[27] Michele, M., Raucoules, D., Rault, C., Aunay, B., Foumelis, M.: Short communication: Potential of sentinel-1 interferometric synthetic aperture radar (insar) and offset tracking in monitoring post-cyclonic landslide activities on réunion. Earth Surface Dynamics **11**(3), 451–458 (2023) https://doi.org/10.5194/esurf-11-451-2023

[28] Copernicus Emergency Management Service: EMSR927: Nepal Flood – Emergency Mapping Activation. European Commission, Copernicus Emergency Management Service; via HDX (2026). https://mapping.emergency.copernicus.eu/activations/EMSR927/

[29] Hersbach, H., Bell, B., Berrisford, P., *et al.*: The era5 global reanalysis. Quarterly Journal of the Royal Meteorological Society **146**(730), 1999–2049 (2020) https://doi.org/10.1002/qj.3803

[30] Istituto Nazionale di Geofisica e Vulcanologia (INGV): Nepal: El INGV aclara que la senal sismica registrada el 26 de agosto no fue generada por un terremoto. INGV press release, 27 August 2026 (2026). https://www.ingv.it/es/prensa-urp/oficina-de-prensa/comunicados-de-prensa/Nepal-El-INGV-aclara-que-la-senal-sismica-registrada-el-26-de-agosto-no-fue-generada-por-un-terremoto

[31] Rather, A.F., *et al.*: Glacial lakes and glofs in a warming himalaya–karakoram region: current understanding, challenges, and the way forward. npj Natural Hazards **3**, 7 (2026) https://doi.org/10.1038/s44304-026-00168-w

[32] Kirschbaum, D., Watson, C.S., Rounce, D.R., Shugar, D.H., Kargel, J.S., Haritashya, U.K., Amatya, P., Shean, D., Anderson, E.R., Jo, M.: The state of remote sensing capabilities of cascading hazards over high mountain asia. Frontiers in

Earth Science **7**, 197 (2019) https://doi.org/10.3389/feart.2019.00197

[33] Allen, S.K., *et al.*: Glacial lake outburst flood risk in the poiqu/bhote koshi/sun koshi river basin in the central himalayas. Science Bulletin **64**(7), 435–445 (2019) https://doi.org/10.1016/j.scib.2019.03.011

[34] Shrestha, F., Steiner, J.F., Shrestha, R., Dhungel, Y., Joshi, S.P., Inglis, S., Ashraf, A., Wali, S., Walizada, K.M., Zhang, T.: A comprehensive and version-controlled database of glacial lake outburst floods in high mountain asia. Earth System Science Data **15**(9), 3941–3961 (2023) https://doi.org/10.5194/essd-15-3941-2023